

# Characterization of Al-4.5%Cu alloy with the addition of silicon carbide and bamboo leaf ash

B. Praveen Kumar, A. Kumar Birru\*

*Department of Mechanical Engineering, National Institute of Technology, Manipur 795004, India*

Received 21 February 2018, received in revised form 8 July 2018, accepted 21 July 2018

## Abstract

The stir-casting method was employed to study the effect of adding silicon carbide and the bamboo leaf ash into the Al-4.5wt.%Cu alloy. The standard procedure was followed in analysing the mechanical behaviour of the fabricated composites on parameters such as density, tensile strength, and hardness. Optical microscope, scanning electron microscope with energy dispersive analysis of X-rays, and X-ray diffraction analysis helped in studying the microstructure of the composites. The study reveals that the reinforcement particles in the matrix alloy were distributed nearly homogeneously, and with a clear interface. The X-ray diffraction patterns indicate the presence of silicon carbide and bamboo leaf ash without an intermetallic reaction. The density of the hybrid composites reduces with the addition of bamboo leaf ash, but porosity increases. The fabricated composites gain in tensile strength and hardness as the reinforcement particles are added, but elongation was decreased.

**Key words:** bamboo leaf ash, silicon carbide, hybrid composite, stir casting, mechanical properties

## 1. Introduction

The global quest for materials that are cost-effective and top-notch, while also possessing a high strength-to-weight ratio, continues unabated. No conventional material entirely fits the bill. The search has, therefore, now long since moved from conventional materials to composites. Conventional materials do not possess the feasible combination of strength, stiffness, and density that the aerospace, automotive and marine industries [1], for instance, are looking for. Among the composites that have already been tested are the metal matrix composites (MMCs) in which ceramic particles are added to conventional alloys. Moreover, among MMCs, aluminium-based alloys (AMMCs) are widely preferred, given their stiffness, strength, low weight, and density [2–4]. The AMMCs are reinforced with SiC, B<sub>4</sub>C, zircon, Al<sub>2</sub>O<sub>3</sub>, and fly ash particles to enhance their mechanical and tribological properties considerably [5]. However, these properties still may not meet the requirements of the industries mentioned above.

AMMCs are further reinforced with more than two

other materials to produce aluminium hybrid metal matrix composites (AHMMCs) [6]. The A16061/WC/Gr hybrid fabricated by Subramanya et al. [7] through the stir-casting process by adding WC and Gr particles enhances the mechanical properties of AMMCs. Miranda et al. [8] compared single reinforced composites such as AlSi/SiC and AlSi/Ti with hybrids such as AlSi/Ti/SiC and concluded that the latter have higher tensile strength. Baradeswaran et al. [9] noted that the mechanical and wear properties of aluminium alloys, AA6061 and AA7075, were enhanced by adding 10 and 5% by weight, respectively, of B<sub>4</sub>C and graphite by liquid casting. Bhargavi and Ramanaiah [10] noted that the tensile strength and hardness of matrix alloy, AA2024, improved with the addition of B<sub>4</sub>C and MoS<sub>2</sub>. Several other researchers have also observed that the properties of AMMCs improve with the addition of hybrid reinforcements [11]. Hybrid composites are therefore better than the single reinforced composites [12, 13]. Several researchers have noted that reinforcements are not only more expensive but are also not readily available in most developing countries. It is, therefore, the need of the hour to de-

\*Corresponding author: tel.: +91-8331866984; e-mail address: [anilbirru@gmail.com](mailto:anilbirru@gmail.com)

Table 1. Chemical composition of Al-4.5wt.% Cu alloy (wt.%)

| Cu   | Mg    | Si    | Fe    | Mn    | Ni    | Pb    | Sn    | Ti    | Zn    | Al      |
|------|-------|-------|-------|-------|-------|-------|-------|-------|-------|---------|
| 4.52 | 0.663 | 0.538 | 0.131 | 0.118 | 0.075 | 0.066 | 0.029 | 0.021 | 0.013 | Balance |

Table 2. Chemical composition of BLA (wt.%)

| SiO <sub>2</sub> | CaO  | K <sub>2</sub> O | C   | Al <sub>2</sub> O <sub>3</sub> | MgO  | Fe <sub>2</sub> O <sub>3</sub> |
|------------------|------|------------------|-----|--------------------------------|------|--------------------------------|
| 76.2             | 6.68 | 5.62             | 4.2 | 4.13                           | 1.85 | 1.32                           |

velop cost-effective composites using agro or industrial waste that is readily available and has lower densities.

Researchers have also observed the strengths and limitations in using agro and industrial waste as reinforcements. Siva Prasad and Chintada [14] avowed that hybrid composites produced with the addition of rice husk ash (RHA) as a secondary reinforcement enhanced their wear resistance and mechanical properties. Alaneme et al. [15] fabricated the Al-Al<sub>2</sub>O<sub>3</sub> composite and the Al-Al<sub>2</sub>O<sub>3</sub>-RHA hybrid composite using the stir casting process and analysed their mechanical properties. They observed that incorporating RHA particles improved the mechanical properties of the hybrid (Al<sub>2</sub>O<sub>3</sub> + RHA) composites more than they improved the single (Al<sub>2</sub>O<sub>3</sub>) reinforced composite. Alaneme et al. [16] also reported that the wear and corrosion resistance of the Al-Mg-Si alloy is enhanced by incorporating both bamboo leaf ash (BLA) and Al<sub>2</sub>O<sub>3</sub> than the single (Al<sub>2</sub>O<sub>3</sub>) reinforced Al-Mg-Si alloy. Several other researchers have also reported that adding agro or industrial waste as complementary reinforcement material enhances the properties of aluminium composite [17]. From the extensive survey, it was noticed that limited research work had been carried out utilizing BLA as complimentary reinforcement and research work on Al-4.5%Cu alloy based hybrid composite reinforcing by BLA as secondary reinforcement not yet tried. The objective of the present study attempted to fabricate aluminium hybrid composites by adding SiC and in the secondary phase, agro waste (BLA).

## 2. Experimental procedure

### 2.1. Materials

Aluminium was selected as the matrix, with Cu consisting of 4.5 % of its weight as a major alloying element, and with density 2.7876 g cm<sup>-3</sup>. The chemical composition was as indicated in Table 1. BLA particles were processed as per the standard procedure, under 75 µm with a density of 1.712 g cm<sup>-3</sup>, and SiC particles with an average size of 35 µm and density

of 3.21 g cm<sup>-3</sup> were selected as strengthening materials. Magnesium was used in ingot form to increase the wetting of the reinforcement particles and matrix alloy while fabricating the composite materials.

### 2.2. Preparation of bamboo leaf ash

BLA was prepared as per the standard procedures described by Alaneme et al. [15, 16]. Dry bamboo leaves were collected from farmlands in Manipur, North East India, and placed in the metallic iron drum to burn in the open air, allowing for complete combustion. On completion of the burning process, the ash was collected and allowed to cool for 24 h. The colour of the leaves changed from yellow to black during the process due to the burning of organic material [18]. The ash was milled and then conditioned with an electric muffle furnace at 650°C for 3 hours to remove carbonaceous materials. The colour of the BLA now transposed from black to greyish white. A sieve shaker was used to ensure the BLA particles were under 75 µm in size.

The BLA particles were then characterized using a scanning electron microscope (SEM) micrograph and with X-ray diffraction (XRD) profile as shown in Figs. 1 and 2. The existence of silicon dioxide (SiO<sub>2</sub>), alumina (Al<sub>2</sub>O<sub>3</sub>), carbon (C), calcium oxide (CaO), potassium oxide (K<sub>2</sub>O), ferric oxide (Fe<sub>2</sub>O<sub>3</sub>) and magnesium oxide (MgO) was detectable in the BLA particles confirmed from XRD profile as shown in Fig. 2. The average size of the particles was found to be 75 µm, and their chemical composition as per XRD investigation of BLA is presented in Table 2. The XRD pattern as shown in Fig. 2 indicates that the peaks of the major constituent belong to SiO<sub>2</sub> as depicted in Table 2. Alaneme et al. [19] prepared BLA as per the standard procedure, also presented similar chemical compositions for BLA.

### 2.3. Composite production

The stir casting method is cost-effective and offers a broad selection of materials with various processing conditions for fabricating the single reinforced and

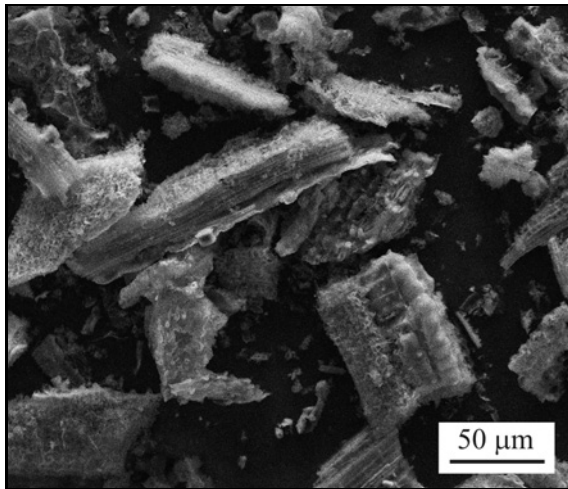


Fig. 1. SEM micrograph of prepared BLA.

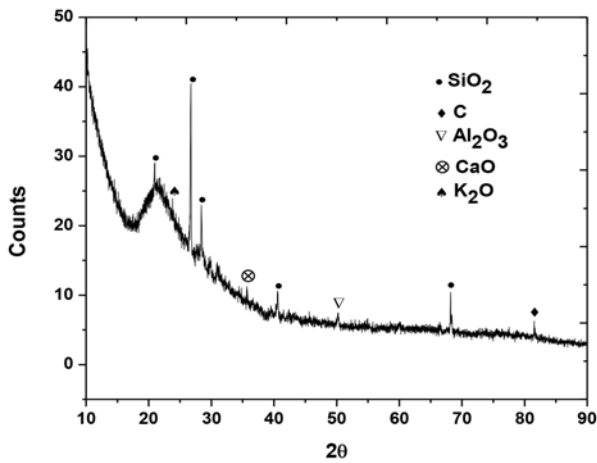


Fig. 2. XRD pattern of prepared BLA.

hybrid reinforced composite. The schematic diagram of stir casting set-up used in the experiment was of the pour-from-the-bottom variety as shown in Fig. 3. The Al-4.5% Cu alloy in the ingot was cut into small pieces and placed in the graphite coated crucible and heated up to 800 °C till the entire alloy melted by using an induction electric resistance furnace. The inert atmosphere was maintained in the melt with argon gas during the operation. The molten metal was al-

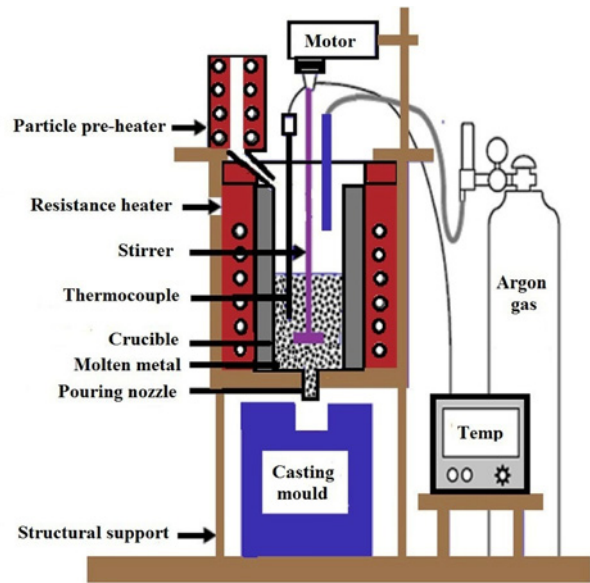


Fig. 3. Schematic diagram of bottom pouring type of stir casting experimental setup.

lowed to cool to 620–650 °C known as the semi-solid state [20] in the furnace. The SiC and BLA particles were preheated at 600 °C to eject the dampness and promote the wettability with the molten alloy.

It is suggested by Hashim et al. [21] that both the matrix and the reinforcement materials be pre-heated at a specific temperature before being mixed to release all the moisture and trapped air between the particles. The heat-treated reinforcement particles were incorporated in the melt, and the magnesium in ingot form approximately 0.1 wt.% is also added to promote wettability between the reinforcements and matrix alloy into the semi-solid state of the molten alloy, and stirring was performed at a speed of 400 rpm about 5–6 min. Then the composite slurry superheated at 750 °C and secondary stirring were executed with mechanical graphite coated stainless steel stirrer. The stirring is performed at a speed of 600 rpm for 10 min to enhance the uniform dispersion of reinforcement particles in the matrix alloy. After incorporating the particles completely, the matrix alloy then poured into the 350 °C preheated permanent steel mould. The fabricated composite material was then fettled at room temperature from the steel mould. The Al-4.5% Cu alloy was fabricated reinforced with single SiC and hy-

Table 3. Details of the fabricated aluminium composites

| Composite code | Composition             | SiC (wt.%) | BLA (wt.%) |
|----------------|-------------------------|------------|------------|
| a              | Al-4.5Cu alloy          | 0          | 0          |
| b              | Al-4.5Cu/10SiC          | 10         | 0          |
| c              | Al-4.5Cu/(10SiC + 2BLA) | 10         | 2          |
| d              | Al-4.5Cu/(10SiC + 4BLA) | 10         | 4          |

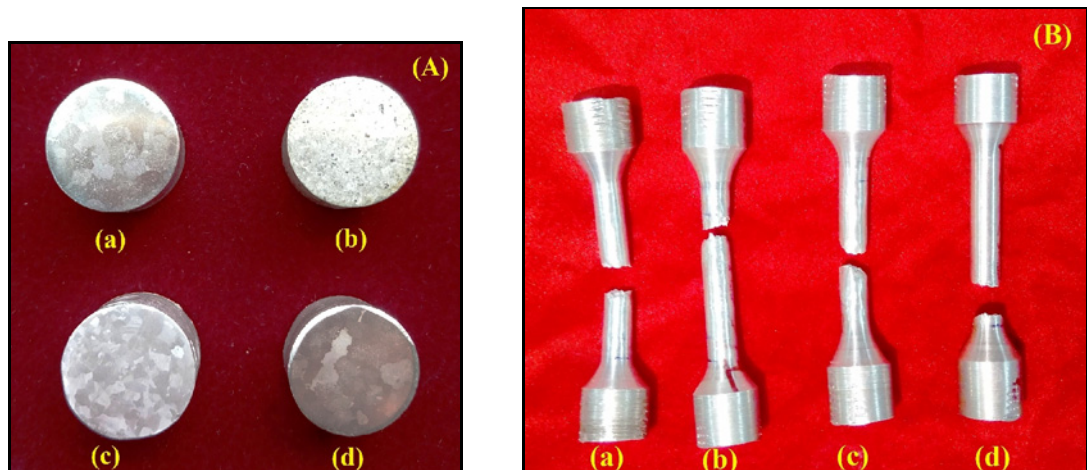


Fig. 4. (A) Macrostructures and (B) fractured tensile test specimens of (a) Al-4.5Cu alloy, (b) Al-4.5Cu/10SiC composite, and (c) Al-4.5Cu/(10SiC + 2BLA) and (d) Al-4.5Cu/(10SiC + 4BLA) hybrid composites.

brid combination (SiC + BLA) as shown in Table 3, and the ingot form was taken. The fabricated composite material was sectioned into samples for microstructure examination, density measurement, and hardness and tensile tests.

#### 2.4. Density and porosity measurements

The density was calculated to determine the porosity levels of the fabricated composites in the stir casting method, and to analyse the influence of the BLA and SiC by weight on the density. Porosity was determined using the different experimental and theoretical densities of each fabricated composite [22]. The experimental density ( $\rho_{\text{ex}}$ ) of the fabricated composites was determined using the water displacement technique (Archimedes' principle) [23] and calculated using the Eq. (1):

$$\rho_{\text{ex}} = \frac{m}{V}, \quad (1)$$

where  $m$  and  $V$  denote the weight of the specimen and the volume of water displaced, respectively. Some porosity may be normal in the fabricated composites because the incorporated particles rise to the contact area on account of air ingested during production. The porosity may play a crucial role in determining the mechanical properties of the fabricated composites. The porosity may not be eliminated during the casting process, though it may be diminished. The porosity of the fabricated composites is determined using the following Eq. (2):

$$\text{Porosity (\%)} = \frac{\rho_{\text{th}} - \rho_{\text{ex}}}{\rho_{\text{th}}} \times 100, \quad (2)$$

where  $\rho_{\text{th}}$  and  $\rho_{\text{ex}}$  denote the theoretical density and experimental density.

Theoretical density ( $\rho_{\text{th}}$ ) may be calculated using the rule of a mixture [24] as given by Eq. (3):

$$\rho_{\text{th}} = \rho_{\text{m}}V_{\text{m}} + \rho_{\text{BLA}}V_{\text{BLA}} + \rho_{\text{SiC}}V_{\text{SiC}}, \quad (3)$$

where  $\rho_{\text{BLA}}$ ,  $\rho_{\text{SiC}}$ ,  $V_{\text{BLA}}$ , and  $V_{\text{SiC}}$  denote the density and volume fraction of BLA and SiC, respectively.

#### 2.5. Microstructure and XRD analysis

The metallographic examination of the fabricated composites was carried out using optical microscopy (OM) and SEM with energy dispersive X-ray spectroscopy (EDX). For the examination of the microstructure, the samples of the fabricated composites were sectioned into slices that were 20 mm by diameter and 15 mm by thickness, as shown in Fig. 4A as macrostructures. All such samples were polished and etched with Keller's reagent (95 ml water, 2.5 ml HNO<sub>3</sub>, 1.5 ml HCl and 1.0 ml HF) [25]. The XRD pattern of the fabricated composites is taken using a Bruker D8 advanced ECO X-ray diffractometer with Cu K $\alpha$ -radiation and Ni filter. The XRD results were examined at a voltage of 40 kV and 25 mA current intensity.

#### 2.6. Hardness and tensile tests

The hardness tests were performed by taking the average of 3 readings for each sample, using micro Vickers hardness machine as per ASTM E384-11 with a load of 500 gm for 15 s and Brinell hardness testing machine as per IS 1500-2005 consisting of ball indenter of 5 mm and a load of 250 kg. The tensile test was performed as per the ASTM B557 standard on the prepared tensile samples. The tensile samples were machined into round shape of 9 mm diameter and 36 mm by gauge length. The tensile tests were

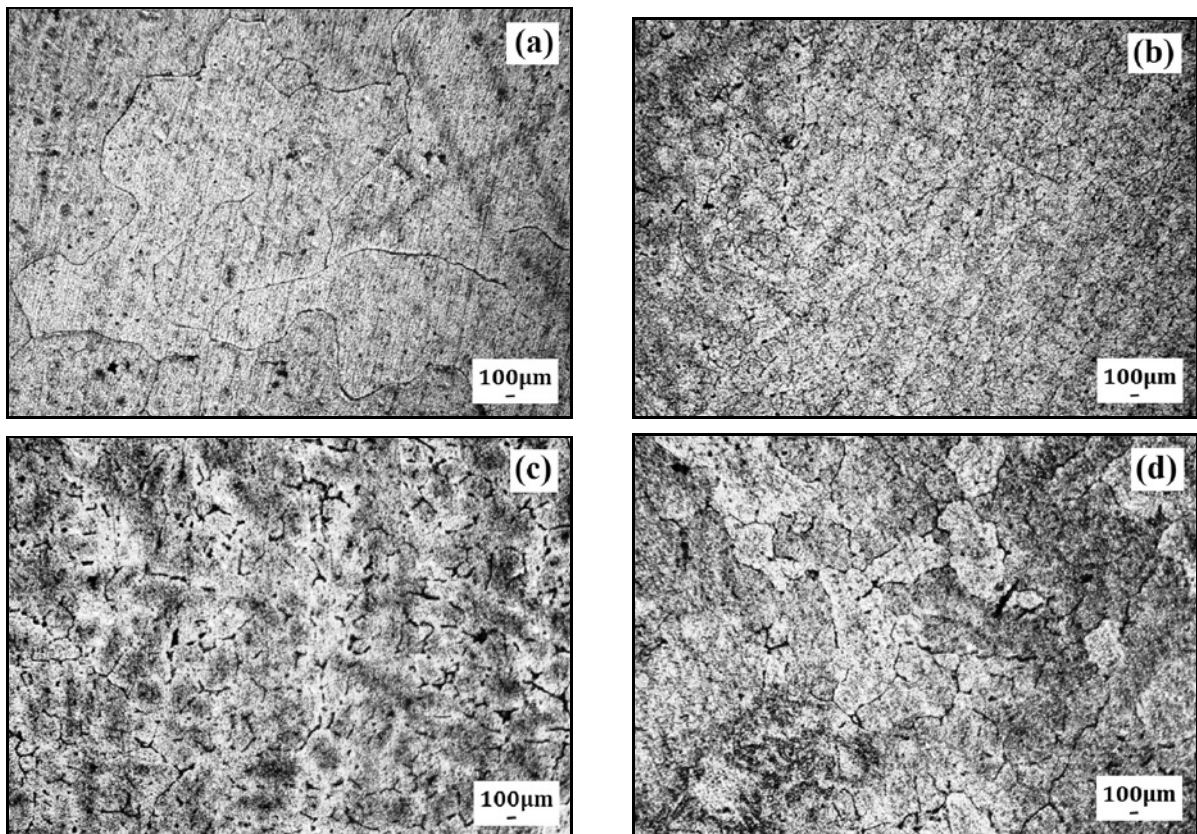


Fig. 5. Optical micrographs of (a) Al-4.5Cu alloy, (b) Al-4.5Cu/10SiC composite, (c) Al-4.5Cu/(10SiC + 2BLA) and (d) Al-4.5Cu/(10SiC + 4BLA) hybrid composites.

conducted using a computerized universal testing machine. The strength and deformability in terms of ultimate tensile strength (UTS), yield strength (YS), and ductility were measured with the tensile test. The break-up of results of the tensile test is as shown in Fig. 4B. The fractured surface of the tensile samples was analysed using SEM investigation.

### 3. Results and discussion

#### 3.1. Microstructure characterization

Among the key factors that impact the properties are density, reinforcement particle distribution, and the microstructure of the composites. The mechanical properties are enhanced with a uniform scattering of the reinforcement particles in the fabricated composites. Variables such as solidification rate, kind of reinforcement and process of incorporation control the distribution of reinforcement particles, preventing them from segregation or agglomeration during the fabrication of the composites. The OM and SEM micrograph of the Al-4.5Cu alloy, Al-4.5Cu/10SiC composite, and Al-4.5Cu/(10SiC + 2BLA) and Al-4.5Cu/(10SiC + 4BLA) hybrid composites are as shown in Figs. 5 and 6. The microstructure of the matrix alloy as shown

in Fig. 5a includes a mixture of primary  $\alpha$ -Al and primary Cu in addition to eutectic phase. Figure 6a shows the SEM micrograph of the matrix alloy and the white phase in the SEM micrograph is the  $\text{Al}_2\text{Cu}$  intermetallic phase.

Figures 5b–d indicate that the average grain size of the matrix is diminished with the incorporation of SiC and BLA particles in the fabricated composites. This is because the reinforcement particles may act as efficient grain refiners. The matrix grain size decreased with the increase in some reinforcement particles and is confirmed by the average grain size measurement conducted by “linear intercept method” which is shown in Fig. 9.

The grains of the fabricated composites were refined, partly because the SiC and BLA particles act as grain nucleation sites, while the matrix grains solidify on them. The solidification process of the composites is influenced by the incorporation of SiC and BLA particles. The distribution of reinforcement particles in the Al-4.5Cu/SiC composite and Al-4.5Cu/(SiC + BLA) hybrid composites prevent the improvement of  $\alpha$ -Al grains in the period of solidification as shown in Fig. 5. The grain nucleation sites are amplified in the fabricated composites. This is because the weight percentage in the reinforcement phase resists the free development of  $\alpha$ -Al grains and further

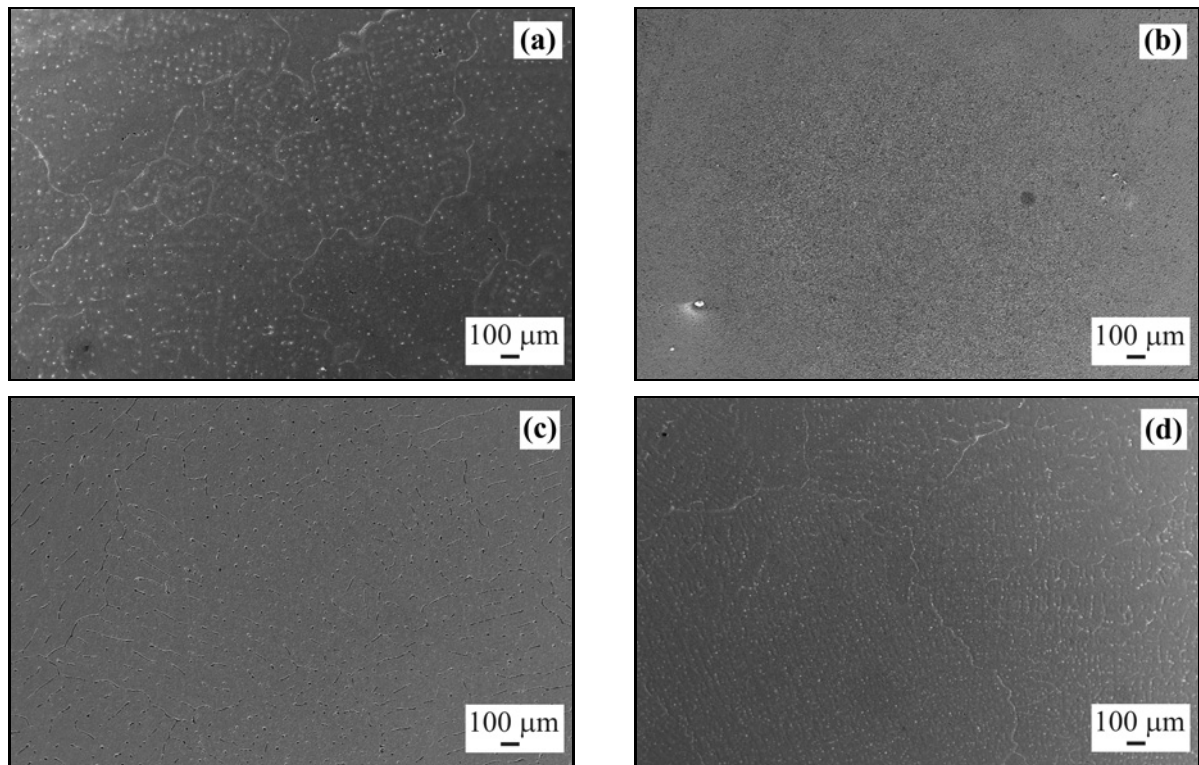


Fig. 6. SEM micrographs of (a) Al-4.5Cu alloy, (b) Al-4.5Cu/10SiC composite, (c) Al-4.5Cu/(10SiC + 2BLA) and (d) Al-4.5Cu/(10SiC + 4BLA) hybrid composites.

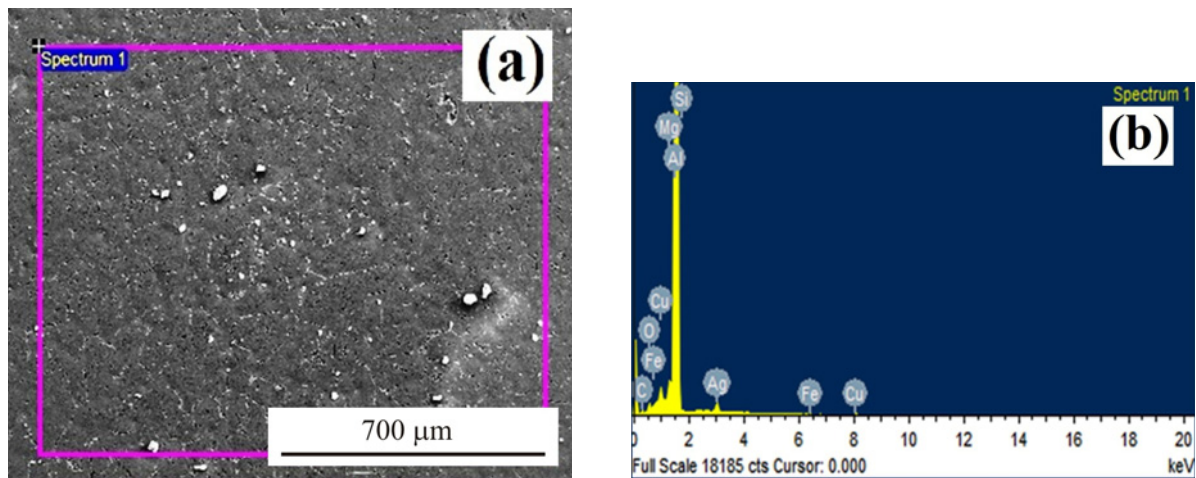


Fig. 7. EDX profile of Al-4.5Cu/(10SiC + 4BLA) hybrid composite.

refines the grains [26]. It is confirmed from Fig. 9. It was observed that with an increase in wt.% of BLA, the grain size of the composites decreased as shown in Fig. 9.

EDX profiles help confirm that the SiC and BLA particles are incorporated uniformly in the fabricated composites, as shown in Fig. 7. The peaks of aluminium (Al), oxygen (O), carbon (C), iron (Fe), silicon (Si), and magnesium (Mg) were detected with wt.% of corresponding elements from the EDX profiles as depicted in Table 4. The existence of these ele-

ments in the fabricated composites confirmed the existence of SiC, silica ( $\text{SiO}_2$ ), alumina ( $\text{Al}_2\text{O}_3$ ), ferric oxide ( $\text{Fe}_2\text{O}_3$ ), and magnesium oxide (MgO), which are elements derived from the BLA as depicted in Table 2. The results confirmed that the reinforcement particles are uniformly dispersed in the matrix as shown in the optical image in Fig. 5 and SEM images in Figs. 6b–d. The uniform dispersion of hard ceramic particles enhances the mechanical properties [27]. The SEM micrographs indicate that the interface between the reinforcement particles and the matrix alloy is clear,

Table 4. The weight per cent of observed elements in Al-4.5Cu/(10SiC + 4BLA) hybrid composite by EDX analysis

|        | C K  | O K  | Mg K | Al K  | Si K | Fe K | Cu L | Ag L | Totals |
|--------|------|------|------|-------|------|------|------|------|--------|
| (wt.%) | 2.81 | 1.18 | 0.48 | 92.29 | 0.12 | 0.07 | 1.37 | 1.67 | 100    |
| (at.%) | 6.18 | 1.95 | 0.52 | 90.22 | 0.12 | 0.03 | 0.57 | 0.41 |        |

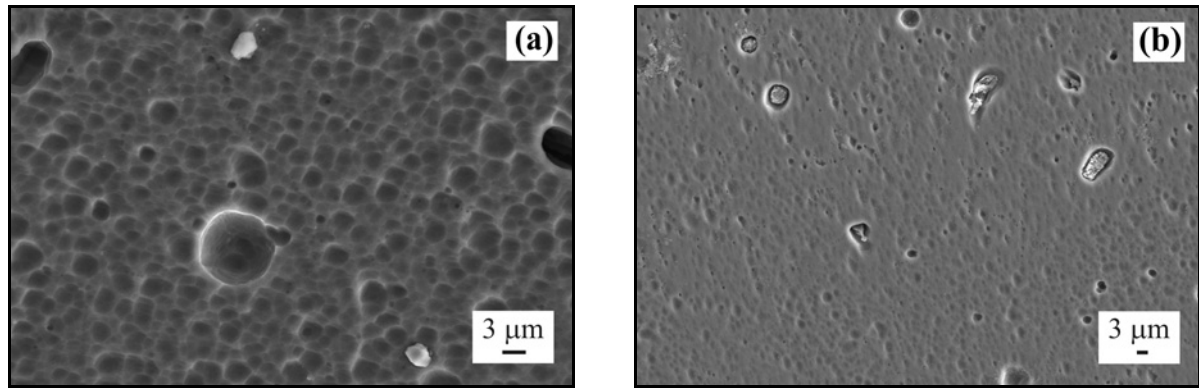


Fig. 8. SEM micrograph of (a) Al-4.5Cu/(10SiC + 2BLA) and (b) Al-4.5Cu/(10SiC + 4BLA) hybrid composites.

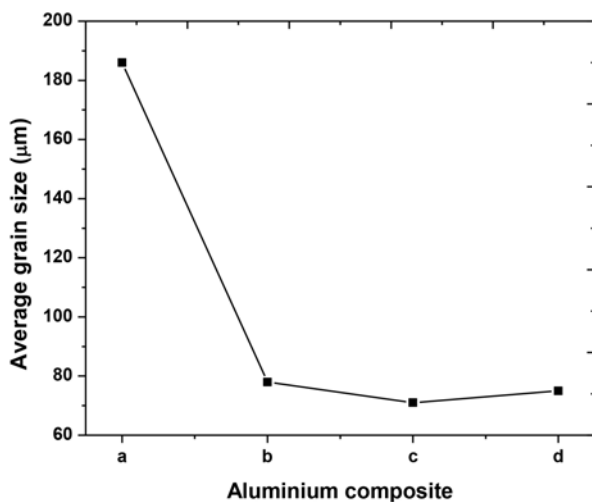


Fig. 9. The average grain size of aluminium composites.

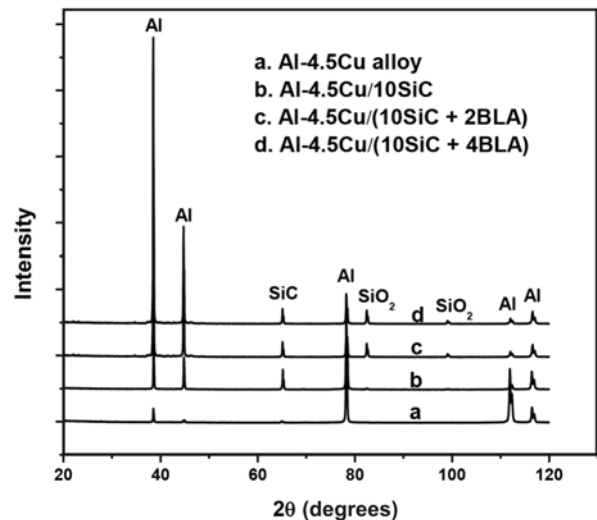


Fig. 10. XRD pattern of fabricated composites.

as shown in Fig. 8. This may, in turn, indicate that the reinforcement particles and the matrix alloy are strongly bonded.

### 3.2. XRD characterization

The XRD patterns of Al-4.5Cu alloy, Al-4.5Cu/10SiC composite, and Al-4.5Cu/(10SiC + 2BLA) and Al-4.5Cu/(10SiC + 4BLA) hybrid composites were as depicted in Fig. 10. The diffraction peaks of SiC and SiO<sub>2</sub> are presented in the fabricated composites. The intensity of SiC and SiO<sub>2</sub> peaks increased with the addition of reinforcement in the fabricated composites. Figure 10 indicates that the aluminium diffrac-

tion peaks are lightly shifted to the lower 2θ of the single and hybrid reinforced composites in comparison with matrix alloy due to the incorporation of SiC and BLA particles in the matrix alloy. It is also observed from Fig. 10 the diffraction peaks of Al, SiC and SiO<sub>2</sub> are present, and other elements were not observed, and it confirms that the integrity of SiC and BLA particles is conserved during casting, SiO<sub>2</sub> is the major constituent in the BLA. The SiC and BLA particles were thermodynamically stable at a temperature of the synthesizing casting. Interfacial reactions were not observed between the matrix and reinforcement particles. These interfacial reactions may lead to the development of brittle intermetallic compounds in the

Table 5. Density and per cent porosity of composites

| Sample code | Composites              | Theoretical density (g cm <sup>-3</sup> ) | Experimental density (g cm <sup>-3</sup> ) | % Porosity |
|-------------|-------------------------|---|--|------------|
| A           | Al-4.5Cu alloy          | 2.7876                                    | 2.7538                                     | 1.212      |
| B           | Al-4.5Cu/10SiC          | 2.8247                                    | 2.7687                                     | 1.98       |
| C           | Al-4.5Cu/(10SiC + 2BLA) | 2.7892                                    | 2.7239                                     | 2.34       |
| D           | Al-4.5Cu/(10SiC + 4BLA) | 2.7546                                    | 2.6829                                     | 2.6        |

fabricated composites, and diminish the properties of the composites. The fabrication of the composite in the stir casting method (reinforcement particles are incorporated in the matrix at semi-solid condition) helps to restrain the interfacial reactions. The potency of the composite is impacted by the nature of the reinforcement particles phase. The findings of the present investigations are consistent with those of earlier researchers [28].

### 3.3. Density and porosity measurement

The density and porosity of the Al-4.5Cu alloy, Al-4.5Cu/10SiC composite, Al-4.5Cu/(10SiC + 2BLA) and Al-4.5Cu/(10SiC + 4BLA) hybrid composites were as depicted in Table 5. The density of the fabricated composite increased with the incorporation of SiC content and reduced with the addition of BLA in hybrid composites in comparison with the matrix alloy as shown in Table 5. The reduced density in the hybrid composite was due to increase in the low-density BLA particles. These results are in line with Alenemi et al. [29] noted that the density of the hybrid composites reduced when reinforcement content was added. The theoretical density of the composites was calculated by the rule of the mixture, using Eq. (3). The porosity of the Al-4.5Cu alloy, single reinforced and hybrid composites was measured based on the theoretical and measured densities using Eq. (2), and it was observed that the porosity increased slightly as depicted in Table 5.

The increase in porosity may be because of the particle-to-particle contact that increases as reinforcement particles are added. The contact of particles with each other may lead to a decrease in the interfacial bonding of reinforcement particles with matrix alloy, which promoted the residual pores in the fabricated composites. Also, gas may be trapped during the stirring: air bubbles enter into the melt either independently or enveloped by the reinforcement particles.

The increment in porosity at 2.6 % of Al-4.5Cu/(10SiC + 4BLA) hybrid composite was observed in comparison with the matrix alloy as shown in Table 5. From these results, it may be concluded that lighter-weight composites may be produced at a significantly reduced cost, a conclusion that Senthilkumar et al. [30] and Dwivedi et al. [31] agree with.

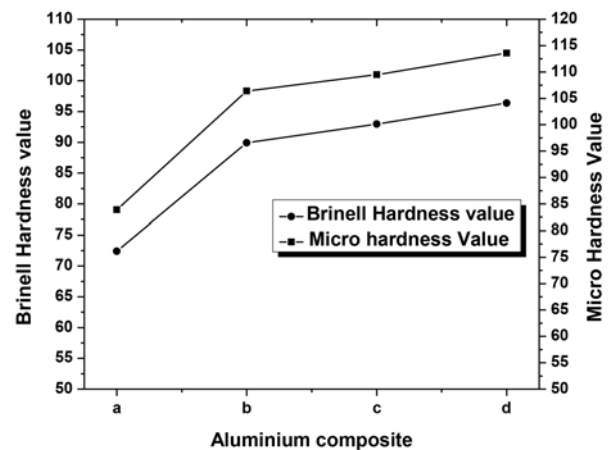


Fig. 11. BHV and MHV of fabricated composites.

### 3.4. Hardness measurement

The hardness values of the Al-4.5Cu alloy and composites were as depicted in Fig. 11. The hardness increased with the addition of reinforcement content. The hardness of single and hybrid reinforced composites was considerably higher than that of the matrix alloy. The highest hardness value was found in the hybrid composite that consisted of 10 wt.% SiC and 4 wt.% BLA, as shown in Fig. 11. The Brinell hardness value (BHV) increased up to 28 %, and microhardness value (MHV) increased up to 32 % in the Al-4.5Cu/(10SiC + 4BLA) hybrid composite in comparison with matrix alloy as shown in Fig. 11. Similar results were observed by Mahendra and Radhakrishna [32] who fabricated the aluminium hybrid composites with the addition at 5, 10, and 15 wt.% (equal proportion) of SiC and fly ash reinforcement particles using the stir casting route, and exhibited higher hardness value. The hardness of the composites increased with the accumulation of SiC and BLA particles. This may be because of the hard nature of ceramic particles, and homogeneous distribution of reinforced particles with good interfacial bonding with the matrix alloy. The grain refinement observed in the composite may be because the reinforcement particles act as effective grain refiners. According to the Hall-Petch relation, the hardness increases with a reduction in grain size [33]. The hardness enhancement of the hybrid compos-

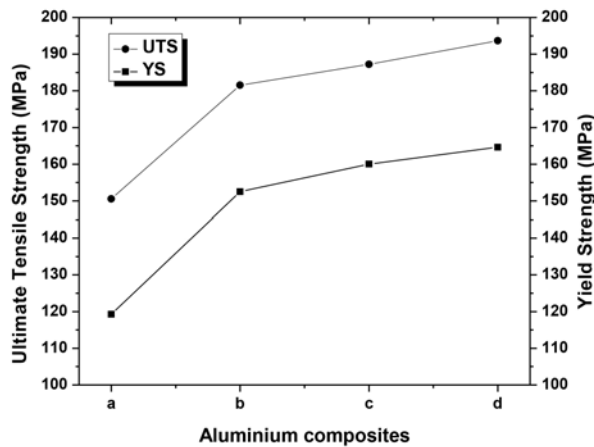


Fig. 12. UTS and YS of fabricated composites.

ite may also be because the reinforcement particles hinder dislocation [34]. Also, the reinforcement particles protect the softer matrix. The hard reinforced particles thus restrict deformation and resist indentation when touched [28]. The increased hardness may also be because SiC and BLA withstand the major load transferred by the matrix.

### 3.5. Tensile behaviour

The tensile behaviour of the fabricated composite was studied as UTS and YS, and ductility in terms of percentage elongation. The tensile failure mechanism was observed with SEM morphologies of the tensile fracture surface.

#### 3.5.1. Ultimate tensile and yield strength

Variations that occur in the UTS and YS of fabricated aluminium composites when SiC and BLA particles are added are as shown in Fig. 12. It was detected that the strength of the fabricated composites increased with the incorporation of reinforcement phase and highest strength was found in the hybrid composite at 10 wt.% SiC and 4 wt.% BLA. The UTS increased up to 28.65 %, and YS increased up to 38.03 % in the Al-4.5Cu/(10SiC + 4BLA) hybrid composite in comparison over the matrix alloy. The tensile strength of fabricated composites is strengthened by the presence of reinforcement particles in the matrix melt, and by grain refinement and the interfacial bond of the hard reinforcements with the softer matrix. Venkatchalam and Kumaravel also observed a similar trend while studying the tensile strength of aluminium composites reinforced with fly ash and SiC, respectively [35].

The numerous strengthening mechanisms of particulate composites were analysed [36]. The strength of the composites rose as the presence of reinforcement

particles increased due to the mechanisms of direct and indirect strengthening as reported by Chawala and Shen [37], and Cho and Gurland [38]. The direct strengthening occurs in the composites with the transfer of load from the softer matrix to the hard ceramic particles through the interface between matrix and reinforcement. The outcome of this principle is that the protection to plastic deformation and work hardening capacity increase in the composites [39]. The indirect strengthening arises in the composites from the thermal mismatch due to uneven cooling between matrix alloy, which has a higher coefficient of thermal expansion (CTE) and ceramic particles with lower CTE [40]. The development of dislocations at the interface between matrix and reinforcement particle occur with a thermal mismatch, a result that is increased in dislocation density that contributes to improving the strength of the composites [37].

The strengthening of the fabricated composites in the present research work may be with the addition of weight fraction of SiC and BLA particles content. The potential direct strengthening effect increased as more SiC particles were added. This may be because the tensile load is transferred from the soft matrix to the hard reinforcement particles since particles act as a barrier to resist the plastic flow when the composite is governed to strain from an applied load [41], as the elastic modulus of SiC is higher than the matrix alloy. Indirect strengthening was also observed in the fabricated composites with the greater difference in the CTE of the ceramic particles and matrix alloy. The strength of the composites increases due to the greater dislocation density [42] arising from the thermal mismatch. In the composite, the extent of dislocation generation is affected by CTE, particle size, particle weight and matrix strength [43]. The CTE value of the matrix alloy and reinforcement particles is different, and the CTE of the matrix alloy is higher than that of the ceramic particles. The CTE of Al-4.5Cu alloy is  $19 \times 10^{-6}$  to  $23 \times 10^{-6} \text{ K}^{-1}$ ; that of SiC is  $4.3 \times 10^{-6}$  to  $4.7 \times 10^{-6} \text{ K}^{-1}$ , and that of SiO<sub>2</sub> is  $0.55 \times 10^{-6}$  to  $0.75 \times 10^{-6} \text{ K}^{-1}$ , which is a major constituent of BLA.

Siva Prasad et al. [44] fabricated aluminium hybrid composites with the addition of rice husk ash (RHA) and SiC by the stir casting route. They ascribed the strengthening effect of the hybrid composite to the rise in dislocation density, caused by the thermal mismatch between matrix and reinforcement. The differences in the CTE construct strain fields around the reinforcement particles in the matrix during solidification. These strain fields obstruct the movement of dislocations while applying the tensile load. A higher load may need to be applied to pass on the dislocations around the strain fields [45]. From the results, it may be concluded that the appraisable strength-to-weight ratio can be enhanced by using cost-effective

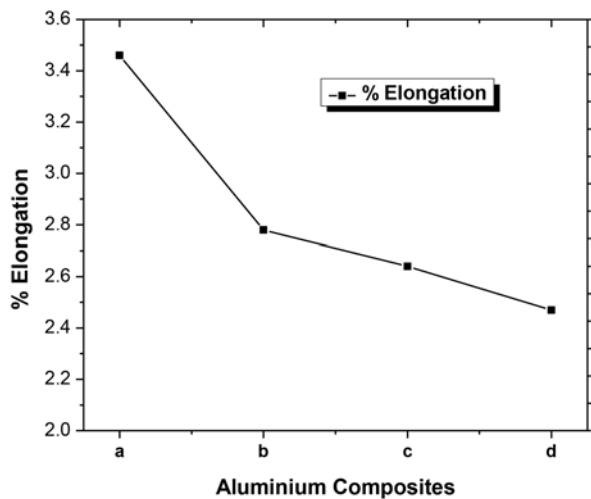


Fig. 13. The percentage of elongation of fabricated composites.

economical agro waste BLA, and SiC as a complementing reinforcement, while fabricating aluminium composites.

### 3.5.2. Ductility

The ductility of the composite materials is ob-

served in terms of the percentage of elongation. The elongation of the fabricated composites diminishes with an addition in the reinforcement percentage as shown in Fig. 13. The percentage of elongation of composites reduces to about 3.46 to 2.47 in the Al-4.5Cu/(10SiC + 4BLA) hybrid composite over the matrix alloy. These findings are well supported by those of previous researchers that the ductility of aluminium composites reduces with the addition of SiC [46], fly ash [47] and bagasse ash [48].

The deterioration in the percentage of elongation is because of the presence of hard ceramic particles. The embrittlement effect may be due to an increase in local stress concentration sites at the interface of matrix alloy and reinforcement particles. Hence, the difference in elastic behaviour between the matrix and reinforcement particles increases. The developing stress field in the matrix and reinforcement particles hinders the passage of dislocations [49]. It is well known that the percentage of elongation reduces as UTS and YS rise. Adding reinforcement particles reduces the elastic deformation, and gradually promotes the plastic deformation in the composites. The presence of hard reinforcement particles tends to result in the formation of cracks, and the subsequent debonding may lead to elastic deformation with increased load. The elongation fracture of the fabricated composites was seen to

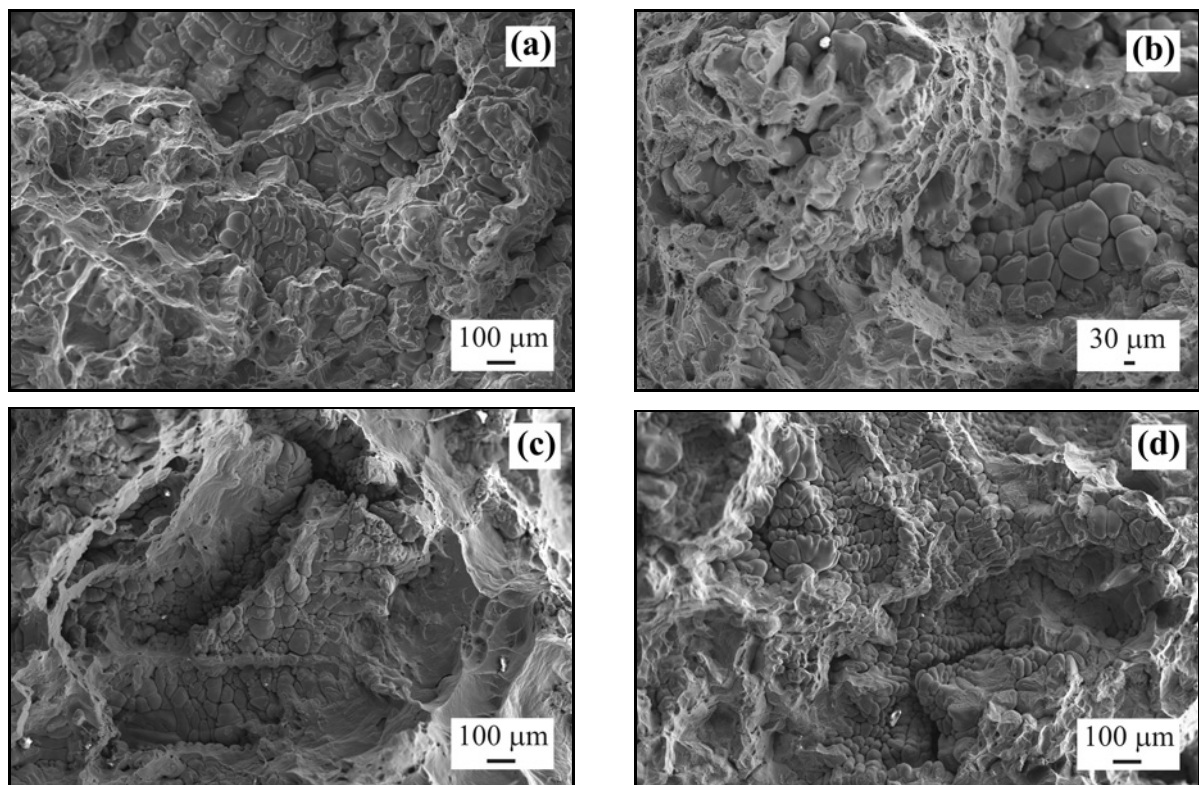


Fig. 14. Tensile fracture morphologies of (a) Al-4.5Cu alloy, (b) Al-4.5Cu/10SiC composite, (c) Al-4.5Cu/(10SiC + 2BLA) and (d) Al-4.5Cu/(10SiC + 4BLA) hybrid composites.

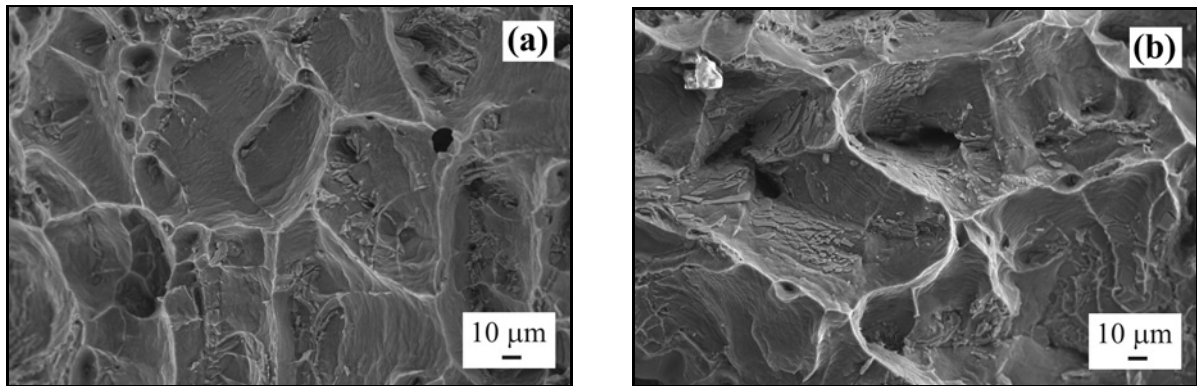


Fig. 15. SEM micrograph of (a) Al-4.5Cu/10SiC composite and (b) Al-4.5Cu/(10SiC + 4BLA) hybrid composite showing the presence of reinforcement particles in the cavities at higher magnification.

reduce, with the addition of reinforcement particles. Localization of the matrix deformation and the fracture of reinforcement particles are key factors that are accountable for the reducing ductility of the composites [50].

### 3.5.3. Fractography and fracture analysis

The failure mechanism during the tensile test of the fractured surfaces of Al-4.5Cu alloy and hybrid composites was subjected to SEM analysis as shown in Fig. 14. The influence of the reinforcement particles on the tensile fracture morphology of the fabricated composites was examined in detail from Figs. 14 and 15. The larger voids are uniformly distributed in the fracture SEM micrograph of the matrix alloy as Fig. 14a indicates. Figure 14a depicts the ductile type of fracture in the matrix alloy due to shearing in the form of dimples, void growth coalescence and ductile failure.

The addition of reinforcements reduces the quantum of voids and dimples as shown in Figs. 14b–d, signifying that elongation reduces, and the tensile strength increases. The brittle fracture becomes evident macroscopically, and ductile fracture is seen microscopically. The dimple sizes reduce due to the refinement of grains in the matrix with the addition of SiC and BLA particles, and in turn, result in decreased ductility [51]. The fracture in composite material may be because of cracks initiated, which subsequently proceeds to the debonded interface among the matrix and ceramic particles. The presence of particles assisted or resisted the crack propagation of the composites. The interfacial nature of the ductile matrix and brittle reinforcement is seen in the fracture morphology of single reinforced composites and hybrid composites at higher magnification, as Figs. 15a,b indicate. The strong bond between matrix and reinforcement particles allows for load transfer from the matrix to the reinforcement particles. The particle cracks seen in Fig. 15a and the ductile shear bands observed in the fracture morphology in Fig. 15b signify that the

composite materials retain some ductility. The reinforcement particles remain intact in the dimples as shown in Fig. 15b, which revealed the better interfacial bonding between matrix alloy and reinforcement particles.

It has been suggested that the microcrack and microvoid development in the composites occurs primarily due to debonding along the reinforcement or matrix interface [37]. The coalescence of these microcracks and microvoids facilitates the fracture of the composites. The composite material exhibited tendencies of brittle behaviour may be due to the presence of brittle ceramic (SiC and BLA) particles.

## 4. Conclusions

The Al-4.5Cu alloy, Al-4.5Cu/10SiC and Al-4.5Cu/(10SiC + 2BLA) and Al-4.5Cu/(10SiC + 4BLA) composites were fabricated by the stir casting method, and the microstructure and mechanical behaviour were investigated. The major conclusions are drawn below:

1. The optical, SEM metallographic study and XRD analysis revealed that the uniform dispersion of SiC and BLA particles was detected in the composites. The density of the hybrid composite reduced with the addition of BLA particles. Conversely, porosity increased.

2. With the addition of reinforcement particles, UTS, YS, and hardness increased significantly. The Al-4.5Cu/(10SiC + 4BLA) hybrid composite exhibited higher UTS, YS, and hardness. The Al-SiC-BLA hybrid composite is ideal in applications where substantial weight reduction is wanted.

3. The percentage of elongation reduced with an increase in SiC and BLA content in the fabricated composites. The hybrid composites demonstrated elongation to a lesser degree than the SiC reinforced composite and matrix alloy.

4. Analysis of the fracture mechanism under SEM

micrographs indicates that the area of dimples on the fractured surface in reinforced composites is smaller than in the matrix alloy. The fracture in the composites is because of the crack in particles that occurs when adding SiC and BLA content. The fracture is seen to be brittle macroscopically, and ductile microscopically.

### Acknowledgements

The authors wish to acknowledge their indebtedness to the National Institute of Technology, Manipur (NITM), Imphal, India, 795004, for the financial support extended to Mr B Praveen Kumar, Full Time Research Scholar, Enrolment Number (15PME004). Thanks are also due to Dr Anil Kumar Birru, Assistant Professor and Head, Department of Mechanical Engineering, NITM, for the invaluable guidance extended.

### References

- [1] Babu Rao, J., Venkata Rao, D., Narasimha Murthy, I., Bhargava, N. R. M. R.: *J. Compos. Mater.*, *46*, 2012, p. 1393. [doi:10.1177/2F0021998311419876](https://doi.org/10.1177/2F0021998311419876)
- [2] Shirvanimoghaddam, K., Karbalaeei, A. M., Abdizadeh, H., Pakseresht, A. H., Abdi, F., Shahbazkhan, A.: *Kovove Mater.*, *53*, 2015, p. 139. [doi:10.4149/km\\_2015\\_3\\_139](https://doi.org/10.4149/km_2015_3_139)
- [3] Dikici, B., Bedir, F., Gavgali, M., Kiyak, T.: *Kovove Mater.*, *47*, 2009, p. 317.
- [4] Bican, O.: *Kovove Mater.*, *52*, 2014, p. 77. [doi:10.4149/km\\_2014\\_2\\_77](https://doi.org/10.4149/km_2014_2_77)
- [5] Zaki, A.: *J. Reinf. Plast. Compos.*, *20*, 2001, p. 921. [doi:10.1177/073168401772678896](https://doi.org/10.1177/073168401772678896)
- [6] Singh, J., Chauhan, A.: *J. Mater. Res. Technol.*, *5*, 2015, p. 159. [doi:10.1016/j.jmrt.2015.05.004](https://doi.org/10.1016/j.jmrt.2015.05.004)
- [7] Veeresh Kumar, G. B., Swamy, A. R. K., Ramesha, A.: *J. Compos. Mater.*, *46*, 2011, p. 2111. [doi:10.1177/2F0021998311430156](https://doi.org/10.1177/2F0021998311430156)
- [8] Miranda, G., Buciumeanu, M., Madeira, S., Carvalho, O., Soares, D., Silva, F. S.: *Composites, Part B*, *74*, 2015, p. 153. [doi:10.1016/j.compositesb.2015.01.007](https://doi.org/10.1016/j.compositesb.2015.01.007)
- [9] Baradeswaran, A., Vettivel, S. C., Elaya Perumal, A., Selvakumar, N., Franklin Issac, R.: *Materials & Design*, *63*, 2014, p. 620. [doi:10.1016/j.matdes.2014.06.054](https://doi.org/10.1016/j.matdes.2014.06.054)
- [10] Bhargavi, R., Ramanaiah, N.: *J. Manuf. Sci. Prod.*, *15*, 2015, p. 339. [doi:10.1515/jmsp-2015-0001](https://doi.org/10.1515/jmsp-2015-0001)
- [11] Sharma, P., Dinesh, K., Sharma, S.: *J. Reinf. Plast. Compos.*, *33*, 2014, p. 2192. [doi:10.1177/2F0731684414556012](https://doi.org/10.1177/2F0731684414556012)
- [12] Elango, G., Raghunath, B. K., Palanikumar, K., Thamizhmaran, K.: *J. Compos. Mater.*, *48*, 2014, p. 2227. [doi:10.1177/2F0021998313496592](https://doi.org/10.1177/2F0021998313496592)
- [13] Hassan, A. M., Tashtoush, G. M., Al-Khalil, J. A.: *J. Compos. Mater.*, *41*, 2007, p. 453. [doi:10.1177/2F0021998306063804](https://doi.org/10.1177/2F0021998306063804)
- [14] Dora Siva, P., Chintada, Sh.: *J. Mater. Res. Technol.*, *3*, 2014, p. 172. [doi:10.1016/j.jmrt.2014.03.004](https://doi.org/10.1016/j.jmrt.2014.03.004)
- [15] Alaneme, K. K., Akintunde, I. B., Peter, A. O., Tolulope, M. A.: *J. Mater. Res. Technol.*, *2*, 2013, p. 60. [doi:10.1016/j.jmrt.2013.03.012](https://doi.org/10.1016/j.jmrt.2013.03.012)
- [16] Alaneme, K. K., Olubambi, P. A., Afolabi, A. S., Bodurin, M. O.: *Int. J. Electrochem. Sci.*, *9*, 2014, p. 5663.
- [17] Bodunrin, M. O., Alaneme, K. K., Chown, L. H.: *J. Mater. Res. Technol.*, *4*, 2015, p. 434. [doi:10.1016/j.jmrt.2015.05.003](https://doi.org/10.1016/j.jmrt.2015.05.003)
- [18] Saravanan, S. D., Senthilkumar, M., Shankar, S.: *Tribol. Trans.*, *56*, 2013, p. 1156. [doi:10.1080/10402004.2013.831962](https://doi.org/10.1080/10402004.2013.831962)
- [19] Alaneme, K. K., Adewuyi, E. O.: *Metall. Mater. Eng.*, *19*, 2013, p. 177.
- [20] Geng, L., Zhang, H.-W., Li, H.-Z., Guan, L.-N., Huang, L.-J.: *Trans. Nonferrous Met. Soc. China*, *20*, 2010, p. 1851. [doi:10.1016/S1003-6326\(09\)60385-X](https://doi.org/10.1016/S1003-6326(09)60385-X)
- [21] Hashim, J., Looney, L., Hashmi, M. S. J.: *J. Mater. Process. Technol.*, *92–93*, 1999, p. 1. [doi:10.1016/S0924-0136\(99\)00118-1](https://doi.org/10.1016/S0924-0136(99)00118-1)
- [22] Khosravi, H., Bakhshi, H., Salahinejad, E.: *Trans. Nonferrous Met. Soc. China*, *24*, 2014, p. 2482. [doi:10.1016/S1003-6326\(14\)63374-4](https://doi.org/10.1016/S1003-6326(14)63374-4)
- [23] Gupta, M., Lai, M. O., Soo, C. Y.: *Mater. Sci. Eng. A*, *210*, 1996, p. 114. [doi:10.1016/0921-5093\(95\)10077-6](https://doi.org/10.1016/0921-5093(95)10077-6)
- [24] Abdizadeh, H., Vajargah, P. H., Baghchesara, M. A.: *Kovove Mater.*, *53*, 2015, p. 319. [doi:10.4149/km\\_2015\\_5\\_319](https://doi.org/10.4149/km_2015_5_319)
- [25] Rajaram, G., Kumaran, S., Srinivasa Rao, T.: *J. Compos. Mater.*, *45*, 2011, p. 2743. [doi:10.1177/2F0021998311410465](https://doi.org/10.1177/2F0021998311410465)
- [26] Han, Y., Liu, X., Bian, X.: *Composites: Part A*, *33*, 2002, p. 439. [doi:10.1016/S1359-835X\(01\)00124-5](https://doi.org/10.1016/S1359-835X(01)00124-5)
- [27] Dhanasekaran, S., Sunilraj, S., Ramya, G., Ravishankar, S.: *Trans. Indian Inst. Met.*, *69*, 2016, p. 699. [doi:10.1007/s12666-015-0542-8](https://doi.org/10.1007/s12666-015-0542-8)
- [28] Moses, J. J., Dinakaran, I., Sekhar, S. J.: *Kovove Mater.*, *54*, 2016, p. 257. [doi:10.4149/km\\_2016\\_4\\_257](https://doi.org/10.4149/km_2016_4_257)
- [29] Alaneme, K. K., Ademilua, B. O., Bodunrin, M. O.: *Tribol. Ind.*, *35*, 2013, p. 25.
- [30] Senthilkumar, M., Saravanan, S. D., Shankar, S.: *J. Compos. Mater.*, *49*, 2014, p. 2241. [doi:10.1177/2F0021998314545185](https://doi.org/10.1177/2F0021998314545185)
- [31] Shashi, P. D., Satpal, S., Raghvendra Kumar, M.: *J. Braz. Soc. Mech. Sci. Eng.*, *37*, 2015, p. 57. [doi:10.1007/s40430-014-0138-y](https://doi.org/10.1007/s40430-014-0138-y)
- [32] Mahendra, K. V., Radhakrishna, K.: *J. Compos. Mater.*, *44*, 2010, p. 989. [doi:10.1177/2F0021998309346386](https://doi.org/10.1177/2F0021998309346386)
- [33] Suryanarayana, C., Mukhopadhyay, D., Patankar, S. N., Froes, F. H.: *J. Mater. Res.*, *7*, 1992, p. 2114. [doi:10.1557/JMR.1992.2114](https://doi.org/10.1557/JMR.1992.2114)
- [34] Baradeswaran, A., Elaya Perumal, A.: *Composites: Part B*, *56*, 2014, p. 464. [doi:10.1016/j.compositesb.2013.08.013](https://doi.org/10.1016/j.compositesb.2013.08.013)
- [35] Venkatachalam, G., Kumaravel, A.: *Polym. Polym. Compos.*, *25*, 2017, p. 203.
- [36] Luster, J. W., Thumann, M., Baumann, R.: *Mater. Sci. Technol.*, *9*, 1993, p. 853. [doi:10.1179/mst.1993.9.10.853](https://doi.org/10.1179/mst.1993.9.10.853)
- [37] Chawla, N., Shen, Y.-L.: *Adv. Eng. Mater.*, *3*, 2001, p. 357. [doi:10.1002/1527-2648\(200106\)3:6%3C357::AID-ADEM357%3E3.0.CO;2-I](https://doi.org/10.1002/1527-2648(200106)3:6%3C357::AID-ADEM357%3E3.0.CO;2-I)

- [38] Cho, K., Gurland, J.: Metall. Trans. A, 19, 1988, p. 2027. [doi:10.1007/BF02645206](https://doi.org/10.1007/BF02645206)
- [39] Milan, M. T., Bowen, P.: J. Mater. Eng. Perform., 13, 2004, p. 775. [doi:10.1361/10599490421358](https://doi.org/10.1361/10599490421358)
- [40] Lalet, G., Kurita, H., Heintz, J.-M., Lacombe, G., Kawasaki, A., Silvain, J.-F.: J. Mater. Sci., 49, 2014, p. 397. [doi:10.1007/s10853-013-7717-7](https://doi.org/10.1007/s10853-013-7717-7)
- [41] Alaneme, K. K., Aluko, A. O.: Scientia Iranica A, 19, 2012, p. 992. [doi:10.1016/j.scient.2012.06.001](https://doi.org/10.1016/j.scient.2012.06.001)
- [42] Vogelsang, M., Arsenault, R. J., Fisher, R. M.: Metall. Trans. A, 17, 1986, p. 379. [doi:10.1007/BF02643944](https://doi.org/10.1007/BF02643944)
- [43] Aikin, R. M.: JOM, 49, 1997, p. 35. [doi:10.1007/BF02914400](https://doi.org/10.1007/BF02914400)
- [44] Dora Siva, P., Shoba, Ch., Ramanaiah, N.: J. Mater. Res. Technol., 3, 2014, p. 79. [doi:10.1016/j.jmrt.2013.11.002](https://doi.org/10.1016/j.jmrt.2013.11.002)
- [45] Xia Zhou, Depeng Su, Chengwei Wu, Liming Liu: J. Nanomater., 2012, Article ID 851862. [doi:10.1155/2012/851862](https://doi.org/10.1155/2012/851862)
- [46] Shashi, P. D., Satpal, S., Raghvendra Kumar, M.: Proc IMechE Part B: J. Eng. Manuf., 232, 2016, p. NP2. [doi:10.1177/0954405416673100](https://doi.org/10.1177/0954405416673100)
- [47] Mahendra Boopathi, M., Arulshri, K. P., Iyandurai, N.: American J. Appl. Sci., 10, 2013, p. 219. [doi:10.3844/ajassp.2013.219.229](https://doi.org/10.3844/ajassp.2013.219.229)
- [48] Aigbodion, V. S., Hassan, S. B., Oghenevweta, J. E.: J. Alloys Compd., 497, 2010, p. 188. [doi:10.1016/j.jallcom.2010.02.190](https://doi.org/10.1016/j.jallcom.2010.02.190)
- [49] Ranganath, G., Sharma, S. C., Krishna, M., Muruli, M. S.: J. Mater. Eng. Perform., 11, 2002, p. 408. [doi:10.1361/105994902770343935](https://doi.org/10.1361/105994902770343935)
- [50] Cheng, S.-L., Yang, G. C., Zhu, M., Wang, J.-C., Zhou, Y.-H.: Trans. Nonferrous Met. Soc. China, 20, 2010, p. 572. [doi:10.1016/S1003-6326\(09\)60180-1](https://doi.org/10.1016/S1003-6326(09)60180-1)
- [51] David Raja, S. J., Robinson Smart, D. S., Dinaharan, I.: Mater. Des., 49, 2013, p. 28. [doi:10.1016/j.matdes.2013.01.053](https://doi.org/10.1016/j.matdes.2013.01.053)